



**HAL**  
open science

# **EVM derivation of multicarrier signals to determine the operating point of the power amplifier considering clipping and predistortion**

Ali Cheaito, Jean-François H elard, Matthieu Cruss iere, Yves Lou et

## **► To cite this version:**

Ali Cheaito, Jean-Fran ois H elard, Matthieu Cruss iere, Yves Lou et. EVM derivation of multicarrier signals to determine the operating point of the power amplifier considering clipping and predistortion. EURASIP Journal on Wireless Communications and Networking, 2016, 2016 (1), 10.1186/s13638-016-0771-5 . hal-01431368

**HAL Id: hal-01431368**

**<https://hal.science/hal-01431368v1>**

Submitted on 21 Dec 2017

**HAL** is a multi-disciplinary open access archive for the deposit and dissemination of scientific research documents, whether they are published or not. The documents may come from teaching and research institutions in France or abroad, or from public or private research centers.


L'archive ouverte pluridisciplinaire **HAL**, est destin ee au d ep ot et  a la diffusion de documents scientifiques de niveau recherche, publi es ou non,  emanant des  tablissements d'enseignement et de recherche fran ais ou  trangers, des laboratoires publics ou priv es.

RESEARCH

Open Access



# EVM derivation of multicarrier signals to determine the operating point of the power amplifier considering clipping and predistortion

Ali Cheaito<sup>1\*</sup> , Jean-François Hélard<sup>1</sup>, Matthieu Crussière<sup>1</sup> and Yves Louët<sup>2</sup>

## Abstract

The high peak-to-average power ratio (PAPR) remains a major drawback of multicarrier modulations. Hence, the nonlinear characteristics of power amplifiers (PA) results in strong distortion and low power efficiency when multicarrier modulations are used. In this paper, the impact of the nonlinearities on the amplified multicarrier signal is analyzed, considering both PAPR limitation using clipping and PA linearization. Therefore, we derive the expression of the error vector magnitude (EVM) of the amplified signal with and without the use of polynomial predistortion and/or clipping techniques. We provide analytical EVM expressions that depend on the PA and predistortion characteristics, as well as the PAPR and the average power of both input and clipped signals. These expressions are general formulas which allow to measure in-band distortion at the PA output. The simulation results show that the proposed expressions present perfect accuracy. Moreover, the trade-off between the PA linearity and efficiency is investigated considering the performance of the clipping and predistortion techniques. An analytical expression which gives the optimal input back-off (IBO) maximizing the PA efficiency with respect to any EVM constraint is provided. Finally, the predistortion complexity is discussed aiming at reducing it with respect to an EVM constraint.

**Keywords:** EVM, PAPR, OFDM, Clipping, Predistortion

## 1 Introduction

Multicarrier modulations are a key technology extensively deployed in wireless communication systems such as WiFi, WiMAX, DVB, and LTE. Furthermore, multicarrier modulations may be a worthy candidate for the next generation (5G) cellular systems. Orthogonal frequency division multiplexing (OFDM) wavelet packets multicarrier modulation (WP-MCM) and filter bank multicarrier (FBMC) are the current state-of-the-art multicarrier techniques. All these techniques suffer from high peak-to-average power ratio (PAPR) of the transmitted signal which prevents to feed the power amplifier (PA) at its optimal point, hereby lowering its power efficiency. Considering the PA characteristics and the PA power efficiency, it is well-known that the closer the average power

of the transmitted signal to the nonlinear zone of the PA characteristics, the higher the PA efficiency. So, a trade-off between the linearity and the efficiency of the PA should be carefully considered. In the literature, one can find two main strategies to deal with this problem: PAPR reduction of the transmitted signal and linearization of the PA. The PAPR reduction approach aims at reducing the dynamic range of the transmitted signal. The most popular PAPR reduction techniques are clipping [1], coding [2], selected mapping (SLM) [3], tone reservation (TR) [4], and active constellation extension (ACE) [5]. The second approach is the linearization which tries to compensate for the nonlinearity of the PA. Among the large variety of linearization techniques, the most popular ones are digital predistortion (DPD) [6], linear amplification with nonlinear component (LINC) [7], and feedback [8]. In our study, we consider the clipping technique as a PAPR reduction technique and the predistortion as a linearization technique. Although PAPR reduction and

\*Correspondence: ali.chaito@hotmail.com

<sup>1</sup>IETR/INSA de Rennes, 20 Ave. des Buttes de Coësmes, Rennes, France  
Full list of author information is available at the end of the article

linearization techniques work in a complementary way [9, 10], it turns out that they are often designed separately and implemented independently in conventional systems [11–16]. Nevertheless, recent studies have investigated some joint design of these techniques in order to enhance their interoperability [17–20]. In this paper, we propose to go a step beyond this strategy by introducing a new adaptive approach which controls the clipping and predistortion functions in a flexible way. Our aim is to maximize the PA efficiency and minimize the predistortion complexity with respect to the linearity constraint, as represented by the error vector magnitude (EVM) of the amplified signal, and according to some predefined parameters. These parameters are the PA characteristics, the transmit power, the PAPR of the input signal, and the target EVM. The EVM is a common figure of merits used to evaluate the quality of communication systems. Indeed, most of wireless communication standards such as the IEEE802.11a standard [21], the IEEE802.16e WiMAX standard [22], and the LTE standard [23] have already specified their requirements in terms of the EVM.

Our objective is to derive a flexible transmitter model able to update its parameters according to incoming requirements and outside environment. Hence, this work is a very important step in the analytical study of the global optimization approach of the transmitter efficiency and linearity.

In this context, we are involved in this paper in the analytical derivation of the EVM of multicarrier signals. In [24, 25], we already derived EVM expressions of clipped predistorted multicarrier signals amplified by Rapp PA model. In this paper, we study the amplitude probability distribution of the signal after applying the clipping technique. After that, we derive the EVM expression of nonlinear amplified multicarrier signals using a memoryless polynomial PA model when clipping is activated or not. Then, we focus on the impact of the predistortion technique on the EVM expression. Once again, we derive the EVM of multicarrier signals when the memoryless polynomial predistortion is activated. Therefore, our first contribution consists in providing EVM expressions as a function of the transmitted power, the clipping threshold, and the PA and predistortion characteristics, as well as the PAPR of the input and clipped signals. As far as theoretical EVM derivations are concerned, some upper-bounds can be found in [26, 27], and other contributions, as [28–30], give closed-form EVM expressions but modeling the RF front end as a simple clipping. To the best of our knowledge, despite numerous studies in the literature about PAPR, no analytical expression of the EVM, taking into account all the above mentioned parameters, exists in the literature. Moreover, we investigate the theoretical analysis of the PA linearity-efficiency and the predistortion complexity. We first examine the

PA linearity-efficiency trade-off. Thereby, we provide an analytical expression which gives the optimal input back-off (IBO) and clipping threshold which must be taken to maximize the PA efficiency for any EVM constraint. Secondly, we discuss the trade-off between the PA linearity and the predistortion complexity aiming at reducing the predistortion complexity with respect to an EVM constraint. Therefore, we seek the optimal configuration of clipping and predistortion which maximizes the PA efficiency taking into account the predistortion complexity and satisfying the EVM constraint.

The remainder of the paper is organized as follows. In Section 2, we introduce our system model. Then, the theoretical derivations of the EVM with the simulation results in both cases without and with predistortion are presented in Section 3 and 4, respectively. Afterwards, the theoretical analysis of the trade-off between the PA linearity-efficiency and the complexity of the predistortion is presented in Section 5. Finally, a conclusion and perspectives are drawn in Section 6.

## 2 System model

Figure 1 represents a simplified block diagram of the transmission chain with clipping and predistortion stages preceding the PA. The multicarrier signal  $x_1(t)$ , generated by the system, becomes  $x_2(t)$  after clipping, and  $x_3(t)$  after the predistortion operation. The output of the PA is  $z(t)$ .

### 2.1 Clipping

One of the major drawbacks of multicarrier waveforms is the high PAPR of the signals obtained in the time domain.

**Definition 1** *The PAPR of a signal is defined as the ratio between the maximum and the average power of the signal over a time interval  $T$ , and is given by*

$$PAPR_{[x]} = \frac{\max_{t \in [0, T]} |x(t)|^2}{E\{|x(t)|^2\}}, \quad (1)$$

where  $E\{\cdot\}$  is the expectation function.

There are many PAPR reduction techniques that aim at reducing the dynamic range of the signal amplitude. Clipping is one of the most used techniques for PAPR reduction due to its simplicity and its straightforward

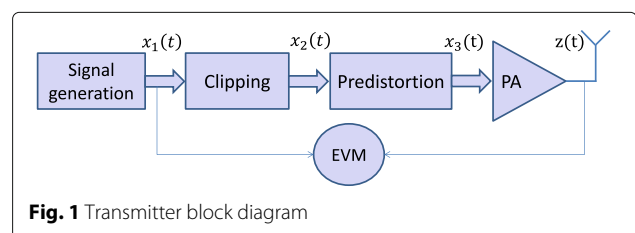


**Fig. 1** Transmitter block diagram

reduction gain. Its main objective is to constraint the high amplitude peaks of a signal to a given threshold  $A_{\max}$ , without affecting the phase  $\phi(x)$ . Thus, the clipped signal,  $x_2(t)$ , is represented as

$$x_2(t) = \begin{cases} x_1(t) & \text{if } |x_1(t)| \leq A_{\max}, \\ A_{\max} e^{j\phi(x)} & \text{if } |x_1(t)| > A_{\max}. \end{cases} \quad (2)$$

This technique results in both in-band and out-of-band distortions because of its nonlinear operation. Additionally, it changes the amplitude probability distribution function of the signal which is discussed in the next subsection.

### 2.2 Signal amplitude distribution after clipping

We assume that the multicarrier signal is characterized by a complex stationary Gaussian process [31]. Therefore, its amplitude converges to a Rayleigh distribution whose probability density function (PDF) can be written as

$$f_{x_1}(r) = \frac{2r}{P_{x_1}} e^{-\frac{r^2}{P_{x_1}}}, \quad (3)$$

where  $P_{x_1}$  is the average power of the input signal  $x_1(t)$  and  $r$  the magnitude of the input voltage, i.e.,  $r = |x_1(t)|$ . However, after clipping, the PDF of the signal amplitude changes and is stated in the following lemma.

**Lemma 1** *The distribution  $f_{x_2}$  of the clipped signal, referring to [31], is expressed as*

$$f_{x_2}(r) = \begin{cases} f_{x_1}(r) & \text{if } |x_2(t)| < A_{\max} \\ \left( e^{-\frac{A_{\max}^2}{P_{x_1}}} - e^{-\frac{r^2}{P_{x_1}}} \right) \delta(r - A_{\max}) & \text{if } |x_2(t)| = A_{\max}, \end{cases} \quad (4)$$

where  $\delta(r)$  is the Dirac delta function and  $PAPR_{[x_1]}$  is the deterministic maximum PAPR value of  $x_1(t)$ . Please note that for a given number of subcarriers and a type of modulation, there is a maximum value that PAPR can reach. For example, given that  $N$  is the number of subcarriers and  $M$ -QAM is the modulation type, the PAPR upper bound is given by  $\frac{3N(\sqrt{M}-1)}{(\sqrt{M}+1)}$ .

*Proof* The proof follows easily from the fact that the signal will not be clipped if  $|x_1(t)| < A_{\max}$ . In this case,  $f_{x_1}(r) = f_{x_2}(r)$ . However, if  $|x_1(t)| > A_{\max}$ , then  $|x_2(t)|$  will be equal to  $A_{\max}$ . Therefore, we obtain

$$f_{x_2}(r) = P\{r > A_{\max}\} \delta(r - A_{\max}), \quad (5)$$

where  $P\{r > A_{\max}\}$  is the probability that  $r$ , the amplitude of  $x_1(t)$ , is larger than the clipping threshold  $A_{\max}$ . Thus, we can write

$$P\{r > A_{\max}\} = \int_{A_{\max}}^{R_{\max}} f_{x_1}(r) dr, \quad (6)$$

where  $R_{\max}$  is the maximum amplitude of  $x_1(t)$ . Hence, calculating the integral in Eq. (6) we get the expression in Eq. (4). Note that the signal amplitude in practice does not tend to infinity and is limited to a maximum value  $R_{\max}$  which depends on the system parameters as the number of subcarriers.  $\square$

The amplitude distribution of the input signal  $x_1(t)$ , and the clipped signal  $x_2(t)$ , are presented in Fig. 2.

Undoubtedly, the average power of the clipped signal,  $P_{x_2}$ , is different from  $P_{x_1}$  as we will see in the following lemma.

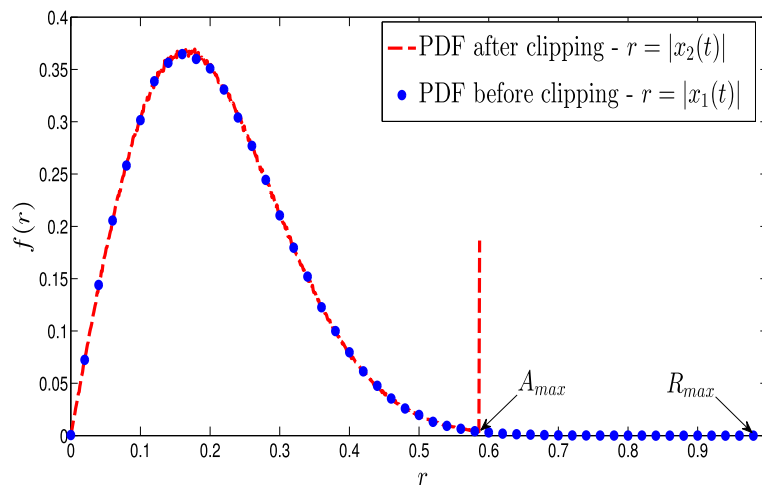


**Fig. 2** Probability density function of the signal amplitude before and after clipping

**Lemma 2** *The ratio  $\lambda$  between the average power after and before clipping is given by*

$$\lambda = \frac{P_{x_2}}{P_{x_1}} = 1 - e^{-\frac{A_{\max}^2}{P_{x_1}}} - \frac{-A_{\max}^2}{P_{x_1}} e^{-PAPR_{[x_1]}} , \quad (7)$$

*Proof*

$$\lambda = \frac{P_{x_2}}{P_{x_1}} = \frac{1}{P_{x_1}} \int_0^{R_{\max}} |x_2(t)|^2 f_{x_2}(r) dr . \quad (8)$$

Substituting the expressions of  $f_{x_2}(r)$  and  $x_2(t)$  into Eq. (8), we show that

$$\begin{aligned} \lambda &= \frac{1}{P_{x_1}} \left( \int_0^{A_{\max}} r^2 f_{x_1}(r) dr + \int_{A_{\max}}^{R_{\max}} A_{\max}^2 f_{x_1}(r) dr \right) \\ &= 1 - e^{-\frac{A_{\max}^2}{P_{x_1}}} - \frac{-A_{\max}^2}{P_{x_1}} e^{-PAPR_{[x_1]}} . \end{aligned} \quad (9)$$

□

Note that the PAPR of the clipped signal,  $PAPR_{[x_2]}$ , is  $\frac{A_{\max}^2}{P_{x_2}}$ . Thus, the ratio  $\frac{A_{\max}^2}{P_{x_1}}$ , which will be used in the following analytical derivations, is equal to  $\lambda$   $PAPR_{[x_2]}$ .

### 2.3 Nonlinear behavioral model of the PA

The PAs used in most of communication systems can be divided basically into two types: the solid state PA (SSPA) and the traveling wave tube amplifier (TWTA). The former, because of its small size, can be used in mobile transmitters, whereas the latter is mostly employed for high-power satellite transponders. In this paper, we consider the SSPA type for a mobile transmitter and assume that it is memoryless and does not present any phase distortion. We represent the AM/AM (amplitude-to-amplitude) characteristic  $H_{PA}(r)$  by the following odd order polynomial<sup>1</sup>

$$H_{PA}(r) = \sum_{l=0}^{L_p-1} b_{2l+1} r^{2l+1}, \quad (10)$$

where  $L_p$  denotes the nonlinear model order,  $b_{2l+1}$  are the nonlinear PA characteristics coefficients, and  $r$  is the amplitude of the input voltage.

### 2.4 Predistortion model

Predistortion is based on the following simple idea: the signal is applied to  $H_{PD}(r)$  which is exactly the inverse of the PA transfer function. Thus, the concatenation of these two functions will ideally be equivalent to a linear function. Since the PA model is a polynomial function, the inverse predistortion function can also be expressed

as a polynomial. Therefore, the predistortion function is expressed as follows

$$H_{PD}(r) = \sum_{k=0}^{K_p-1} a_{2k+1} r^{2k+1}, \quad (11)$$

with  $K_p$  the nonlinear model order and  $a_{2k+1}$  the nonlinear polynomial coefficients.

### 2.5 EVM definition

The error vector magnitude (EVM) is a metric which measures the distortion level of a signal. A signal sent by an ideal transmitter would have all constellation points precisely at their ideal locations. However, various imperfections in the implementation such as the nonlinearity of the PA function and the PAPR reduction stage cause the actual constellation points to deviate from the ideal locations. Figure 3 represents  $X_k$  and  $Z_k$  the  $k$ th complex symbols of the signal before clipping and after amplification,  $x_1(t)$  and  $z(t)$ , respectively. In this figure, a unitary amplification gain is assumed for the clarity of the representation. Note that thanks to the Parseval's theorem which state that the sum (or integral) of the square of a function is equal to the sum (or integral) of the square of its Fourier transform, we can emphasize that the calculation of the EVM can equivalently been led in time or frequency domains. In the sequel, EVM derivations will be based on the following definition of the EVM in the time domain.

**Definition 2** *The EVM is defined as the ratio of the root mean square (RMS) of the difference between a collection of measured symbols and ideal symbols to the root of the mean signal power. Therefore, the EVM of the amplified signal  $z(t)$  is expressed as follows*

$$EVM = \sqrt{\frac{E \{ |z(t) - x_1(t)|^2 \}}{E \{ |x_1(t)|^2 \}}}, \quad (12)$$

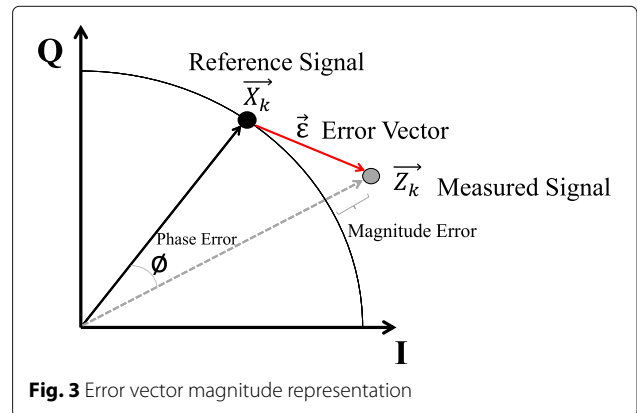


**Fig. 3** Error vector magnitude representation

where

$$E\{|z(t) - x_1(t)|^2\} = \int_0^{R_{\max}} |\epsilon(r)|^2 f_{x_1}(r) dr, \quad (13)$$

with  $\epsilon(r)$  the stationary random variable modeling the signal error and  $f_{x_1}(r)$  the PDF of the amplitude of signal  $x_1$  as defined in Eq. (3). Then, Eq. (13) represents the second order moment of the magnitude error  $|\epsilon(r)|$  and  $E\{|x_1(t)|^2\}$  is the average signal power.

### 3 EVM expressions without predistortion

In this section, we present the results of the EVM derivations when predistortion is not activated, in both cases with and without clipping, as a function of the PA characteristics, the average power and the PAPR of both input and clipped signals.

#### 3.1 Analytical EVM derivations

##### 3.1.1 Without clipping

Firstly, we start by deriving the EVM expression when clipping and predistortion are deactivated. Using Eqs. (3), (10), and (12), we derive a closed-form expression of the EVM. Our main result is presented in the following theorem.

**Theorem 1** *The EVM of an amplified multicarrier signal is expressed as follows*

$$\begin{aligned} \text{EVM} = & \left[ P_{x_1}^{\frac{s-3}{2}} \sum_{p_1+p_3+\dots+p_{2L_p-1}=2} \binom{2}{p_1, p_3, \dots, p_{2L_p-1}} \right. \\ & \left. \times \prod_{l=0}^{L_p-1} (C_{2l+1})^{p_{2l+1}} \times \gamma\left(\frac{s+1}{2}, \text{PAPR}_{[x_1]}\right) \right]^{\frac{1}{2}}, \end{aligned} \quad (14)$$

where  $\gamma$  represents the incomplete gamma function defined as in (43) (see Appendix 1), with

$$s = \sum_{l=0}^{L_p-1} (2l+1) p_{2l+1} + 1, \quad (15)$$

$$\binom{2}{p_1, p_3, \dots, p_{2L_p-1}} = \frac{2!}{p_1! p_3! \dots p_{2L_p-1!}}, \quad (16)$$

and

$$C_{2l+1} = \begin{cases} b_1 - 1 & \text{if } l = 0, \\ b_{2l+1} & \text{if } l \neq 0. \end{cases} \quad (17)$$

Note that the sum in (14) is taken over all combinations of nonnegative integer exponents  $p_1$  through  $p_{2L_p-1}$  such that the sum of all  $p_{2l+1}$  is equal to 2.

*Proof* See Appendix 1. □

This theorem provides an analytical EVM expression in the form of a series expansion involving gamma functions and depending on different parameters. We can see that the in-band distortion of the amplified signal depends on the PA characteristics, as well as the PAPR of the signal  $x_1(t)$  and the average power  $P_{x_1}$ . Note that this expression will be useful in the following analytical derivations of the EVM with clipping.

##### 3.1.2 With clipping

We now lead the EVM calculation considering that the clipping is activated. In this case, using Lemma 1, Lemma 2, Eq. (10), and Eq. (12), we derive a closed-form expression of the EVM which is presented in the following theorem.

**Theorem 2** *The EVM of an amplified multicarrier signal, when clipping is activated, is expressed as follows*

$$\begin{aligned} \text{EVM} = & \left[ -\frac{2H_{PA}(A_{\max})}{\sqrt{P_{x_1}}} \left( \gamma\left(\frac{3}{2}, \text{PAPR}_{[x_1]}\right) - \gamma\left(\frac{3}{2}, \lambda \text{PAPR}_{[x_2]}\right) \right) \right. \\ & + e^{-\lambda \text{PAPR}_{[x_2]}} \times \left( \lambda \text{PAPR}_{[x_2]} + \frac{H_{PA}(A_{\max})^2}{P_{x_1}} + 1 \right) \\ & - e^{-\text{PAPR}_{[x_1]}} \left( \text{PAPR}_{[x_1]} + \frac{H_{PA}(A_{\max})^2}{P_{x_1}} + 1 \right) \\ & + P_{x_1}^{\frac{s-3}{2}} \sum_{p_1+\dots+p_{2L_p-1}=2} \binom{2}{p_1, \dots, p_{2L_p-1}} \prod_{l=0}^{L_p-1} (C_{2l+1})^{p_{2l+1}} \gamma \\ & \left. \times \left( \frac{s+1}{2}, \lambda \text{PAPR}_{[x_2]} \right) \right]^{\frac{1}{2}}, \end{aligned} \quad (18)$$

with

$$s = \sum_{l=0}^{L_p-1} (2l+1) p_{2l+1} + 1, \quad (19)$$

*Proof* See Appendix 2. □

Eventually, as in the case without clipping, Theorem 2 gives an EVM expression in the form of a series expansion composed of Gamma functions and depending on several parameters. These parameters are the PA order  $L_p$ , the PA coefficients  $b_{2l+1}$ , the average power and the PAPR of both input and clipped signals, as well as, the clipping threshold, and  $\lambda$  the ratio between  $P_{x_2}$  and  $P_{x_1}$ .

### 3.2 Simulation results and analysis

In this subsection, we present a comparison between the theoretical EVM, given by Theorem 1 and Theorem 2, and



the simulated EVM when clipping is activated or not. Note that each simulation considers  $10^5$  randomly generated OFDM symbols with 1024 subcarriers associated to 16-QAM modulation symbols. The polynomial coefficients  $b_{2l+1}$  of the PA function have been derived by identification of two AM/AM characteristic. The first one is for a Rapp's SSPA model with knee factor  $p = 2$  and the second one is a real PA for digital video broadcasting-terrestrial (DVB-T). It is designed for use in the 174 to 230 MHz VHF broadcast band, where it can deliver 50 W [33]. Figure 4 represents the gain and power efficiency of a real DVB-T PA as a function of the output power at 202 MHz. We use a high-order polynomial function ( $L_p = 6$ ) to achieve a satisfactory fitting accuracy. Figures 5 and 6 depict the theoretical and simulated EVM as a function of the input power back-off (IBO) when clipping is activated or not using a Rapp-modeled PA and DVB-T PA, respectively. We consider clipping thresholds  $\frac{A_{max}^2}{P_r}$  of 5, 6, 7, and 8 dB. From the curves in Figs. 5 and 6, it can be verified that the more the clipping threshold decreases, the more the EVM increases. In addition, one can notice that using the Rapp-modeled PA, the EVM tends to be zero for high IBO when clipping is deactivated. However, such a behavior is not observed in the case of the DVB-T PA. This is due to the nonlinear characteristics of the DVB-T PA even within the expected linear region, which results in additional distortion. Finally, from the comparison between the theoretical and simulated curves, we conclude that our analytical results in Theorem 1 and Theorem 2 perfectly match the simulated EVM for both PAs. This proves the accuracy of our proposed analytical EVM derivations with and without clipping.

#### 4 EVM expressions with predistortion

In this section, we assume that the predistortion technique is activated. Hence, we investigate the EVM calculation, in both cases with and without clipping, based on the PA characteristics, the predistortion characteristics, and the clipping threshold, as well as the average power and the PAPR of both input and clipped signals. Thus, the equivalent transfer function of the predistortion and amplification stages will be denoted by  $H_{EQ}$ ,

$$H_{EQ}(r) = H_{PA}(H_{PD}(r)). \tag{20}$$

#### 4.1 Analytical EVM derivations

##### 4.1.1 Without clipping

In this case, using Eqs. (3), (12), and (20), we calculate the analytical EVM expression and the solution is given in Theorem 3.

**Theorem 3** *The EVM of a predistorted amplified multi-carrier signal is given by*

$$EVM = \left[ \sum_{p_1+\dots+p_{2L_p-1}=2} \binom{2}{p_1, \dots, p_{2L_p-1}} \prod_{l=0}^{L_p-1} (b_{2l+1})^{p_{2l+1}} \sum_{q_1+\dots+q_{2K_p-1}=m} \binom{m}{q_1, \dots, q_{2K_p-1}} P_{x_1}^{\frac{m}{2}-1} \gamma \left( \frac{m}{2} + 1, \text{PAPR}_{[x_1]} \right) \prod_{k=0}^{K_p-1} (a_{2k+1})^{q_{2k+1}} - e^{-\text{PAPR}_{[x_1]}} (\text{PAPR}_{[x_1]} + 1) + 1 - 2 \sum_{l=0}^{L_p-1} b_{2l+1} \sum_{q_1+\dots+q_{2K_p-1}=2l+1} \binom{2l+1}{q_1, \dots, q_{2K_p-1}} P_{x_1}^{\frac{2l+1}{2}-1} \gamma \left( \frac{2l+1}{2} + 1, \text{PAPR}_{[x_1]} \right) \prod_{k=0}^{K_p-1} (a_{2k+1})^{q_{2k+1}} \right]^{\frac{1}{2}}, \tag{21}$$

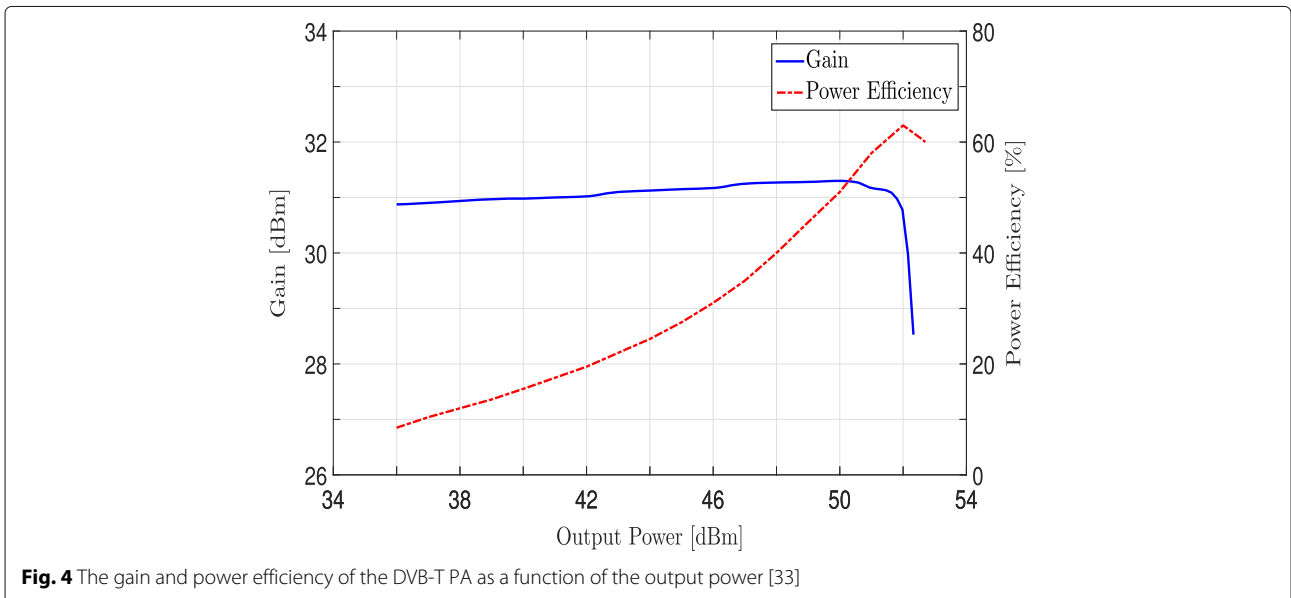


**Fig. 4** The gain and power efficiency of the DVB-T PA as a function of the output power [33]

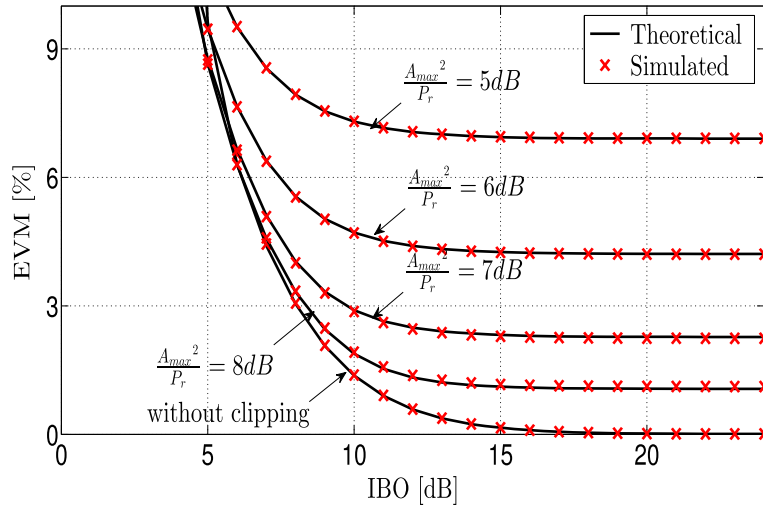


**Fig. 5** Theoretical and simulated EVM without predistortion as a function of the IBO, when clipping is activated or not, using a Rapp modeled PA with  $L_p = 6$

where

$$s = \sum_{k=0}^{K_p-1} (2k + 1) q_{2k+1} + 1, \tag{22}$$

$$m = \sum_{l=0}^{L_p-1} (2l + 1) p_{2l+1}, \tag{23}$$

$$n = \sum_{k=0}^{K_p-1} (2k + 1) q_{2k+1}. \tag{24}$$

*Proof* See Appendix 3. □

As in the case without predistortion, this theorem provides an EVM expression in the form of a series expansion based on gamma functions. Besides, it now depends on the order and coefficients of both the predistortion and the amplifier, as well as the PAPR of the input signal  $x_1(t)$  and its average power  $P_{x_1}$ .

#### 4.1.2 With clipping

In this subsection, we derive the EVM expression when both clipping and predistortion techniques are activated using Eqs. (12) and (20), Lemma 1, and Lemma 2.

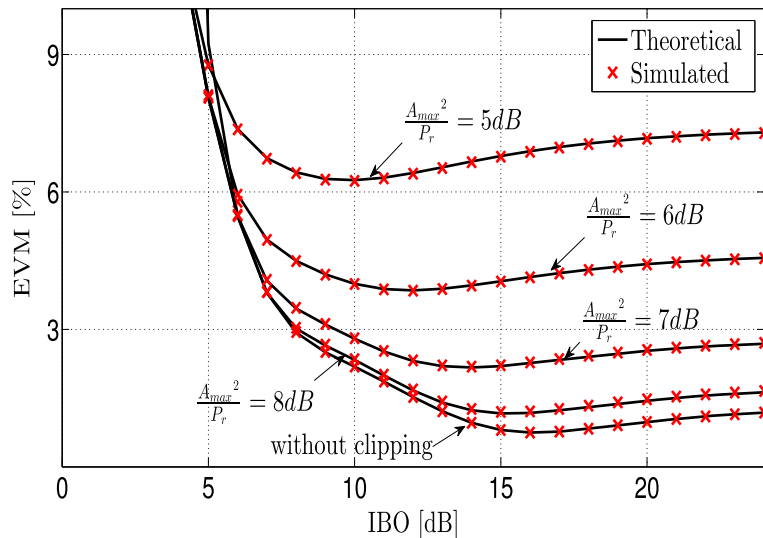


**Fig. 6** Theoretical and simulated EVM without predistortion as a function of the IBO, when clipping is activated or not, using a DVB-T PA with  $L_p = 6$  [33]



**Theorem 4** *The EVM of an amplified multicarrier signal when clipping and predistortion are activated is expressed as follows*

$$\begin{aligned}
 EVM = & \left[ -2 \sum_{l=0}^{L_p-1} b_{2l+1} \sum_{q_1+\dots+q_{2K_p-1}=2l+1} \binom{2l+1}{q_1, \dots, q_{2K_p-1}} \right. \\
 & \times P_{x_1}^{\frac{s}{2}-1} \gamma \left( \frac{s+3}{2}, \lambda \text{PAPR}_{[x_2]} \right) \times \prod_{k=0}^{K_p-1} (a_{2k+1})^{q_{2k+1}} \\
 & - \frac{2H_{EQ}(A_{\max})}{\sqrt{P_{x_1}}} \left( \gamma \left( \frac{3}{2}, \text{PAPR}_{[x_1]} \right) - \gamma \left( \frac{3}{2}, \lambda \text{PAPR}_{[x_2]} \right) \right) \\
 & + \sum_{p_1+\dots+p_{2L_p-1}=2} \binom{2}{p_1, \dots, p_{2L_p-1}} \prod_{l=0}^{L_p-1} (b_{2l+1})^{p_{2l+1}} \\
 & \times \sum_{q_1+\dots+q_{2K_p-1}=m} \binom{m}{q_1, \dots, q_{2K_p-1}} \times \gamma \left( \frac{s}{2} + 1, \lambda \text{PAPR}_{[x_2]} \right) \\
 & \times P_{x_1}^{\frac{s}{2}-1} \prod_{k=0}^{K_p-1} (a_{2k+1})^{q_{2k+1}} - e^{-\text{PAPR}_{[x_1]}} \left( 1 + \frac{H_{EQ}(A_{\max})^2}{P_{x_1}} \right. \\
 & \left. + \text{PAPR}_{[x_1]} \right) + 1 + e^{-\lambda \text{PAPR}_{[x_2]}} \left( \frac{H_{EQ}(A_{\max})^2}{P_{x_1}} \right) \\
 & - 2 \sum_{l=0}^{L_p-1} b_{2l+1} \sum_{q_1+\dots+q_{2K_p-1}=2l+1} \binom{2l+1}{q_1, \dots, q_{2K_p-1}} \\
 & \left. \times P_{x_1}^{\frac{s}{2}-1} \gamma \left( \frac{s}{2} + 1, \lambda \text{PAPR}_{[x_2]} \right) \prod_{k=0}^{K_p-1} (a_{2k+1})^{q_{2k+1}} \right]^{1/2}, \quad (25)
 \end{aligned}$$

where

$$s = \sum_{k=0}^{K_p-1} (2k+1) q_{2k+1} + 1, \quad (26)$$

$$m = \sum_{l=0}^{L_p-1} (2l+1) p_{2l+1}, \quad (27)$$

$$n = \sum_{k=0}^{K_p-1} (2k+1) q_{2k+1}. \quad (28)$$

*Proof* See Appendix 4.  $\square$

Eventually, as in the case without clipping, Theorem 4 gives an EVM expression in the form of a series expansion depending on the same parameters. In addition, it now depends on the PAPR of the clipped signal  $x_2(t)$ , the clipping threshold, and  $\lambda$  the ratio between  $P_{x_2}$  and  $P_{x_1}$ .

## 4.2 Simulation results and analysis

In this subsection, we present a comparison between the theoretical EVM, given by Theorem 3 and Theorem 4, and the simulated EVM when predistortion is activated. Figures 7 and 8 depict the theoretical and simulated EVM as a function of the IBO when clipping is activated or not using the previously introduced Rapp-modeled and DVB-T PAs, respectively. We consider the predistortion order  $K_p = 5$  and clipping thresholds  $\frac{A_{\max}^2}{P_r}$  of 5, 6, 7, and 8 dB. Note that the indirect learning is used to extract the coefficients  $a_{2k+1}$  [34]. First of all, we can see from the curves in Figs. 7 and 8 that the EVM of the predistorted and amplified signal in the case of DVB-T PA is similar to the EVM in the case of a modeled PA. This is due to the high linearization order which provides a linear response of the transmitter chain in both cases. In addition, we remark that the lower the clipping threshold, the higher the EVM. We note also that the EVM increases rapidly when the IBO

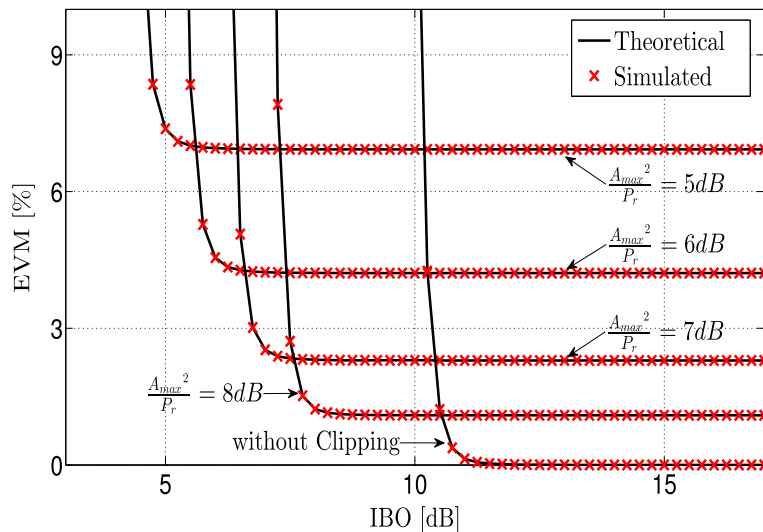


**Fig. 7** Theoretical and simulated EVM with predistortion as a function of the IBO, when clipping is activated or not, using a modeled PA with  $L_p = 6$  and  $K_p = 5$

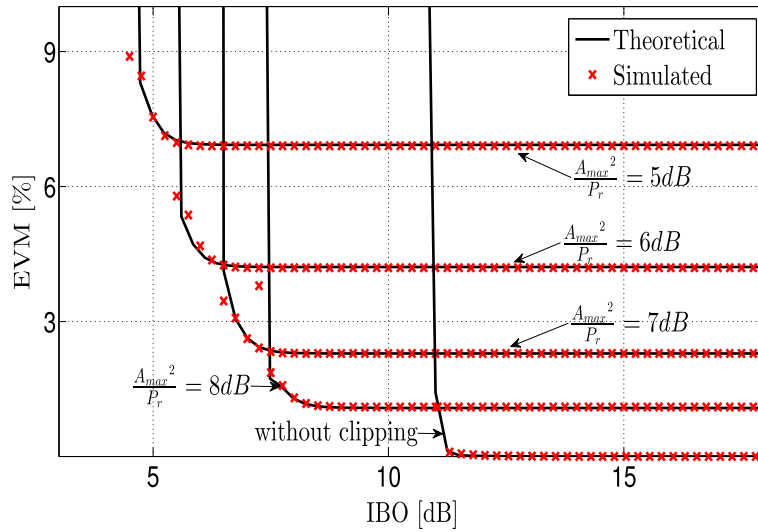


**Fig. 8** Theoretical and simulated EVM with predistortion as a function of the IBO, when clipping is activated or not, using a DVB-T PA with  $L_p = 6$  and  $K_p = 5$  [33]

is lower than the clipping threshold. This is explained by the fact that the peaks of the signal are amplified in the saturation zone of the PA. Once again, we can observe that the theoretical curves perfectly match the simulated ones validating the consistency and accuracy of the proposed EVM expressions.

**5 Theoretical analysis of the trade-off between PA linearity-efficiency and predistortion complexity**

In the previous section, we have analytically proven that the linearity of the PA measured by the EVM metric depends on the performance of clipping and predistortion. In this section, we show that the performance of clipping and predistortion also impacts the PA’s efficiency. Thus, we theoretically analyze the trade-off between the PA linearity and efficiency considering the clipping and predistortion techniques. Secondly, as far as the complexity and the power consumption of the digital signal processing in the baseband are concerned, we expand our study to minimize the complexity of the predistortion technique with respect to an EVM constraint. Therefore, we seek to provide a joint configuration of the predistortion and clipping techniques which maximizes the PA power efficiency taking into account the complexity of the predistortion technique and considering an EVM constraint.

**5.1 Definition of PA efficiency**

According to [35], the PA accounts for 55–60% of the overall power consumption at full load in a LTE macro base station. Thus, its efficiency has a key role in the energy efficiency of the transmitter chain. Referring to Fig. 9, the

PA power efficiency  $\eta_{DC}$  is defined as the ratio between the output power  $P_{out}$  and the DC power  $P_{DC}$ .

$$\eta_{DC} = \frac{P_{out}}{P_{DC}} \tag{29}$$

In [36], the author proposed a relationship that gives the efficiency of the PA (so of classes A, B, and AB) as a function of the output power back-off (OBO). This relationship is given by

$$\eta_{DC} = \beta \frac{1}{OBO} \tag{30}$$

where  $\beta$  equals 0.50, 0.66, and 0.78 for classes A, AB, and B PAs, respectively. In Fig. 10, the power efficiency in Eq. (30) is plotted versus the OBO for classes A, B, and AB PAs. Since, the relationship between OBO and IBO is proportional, we can notice that the more the IBO decreases, the more the efficiency increases. However, from Figs. 6 and 8, as expected, we note that the more the IBO decreases, the more the EVM increases. This means that the linearity is degraded while the power efficiency

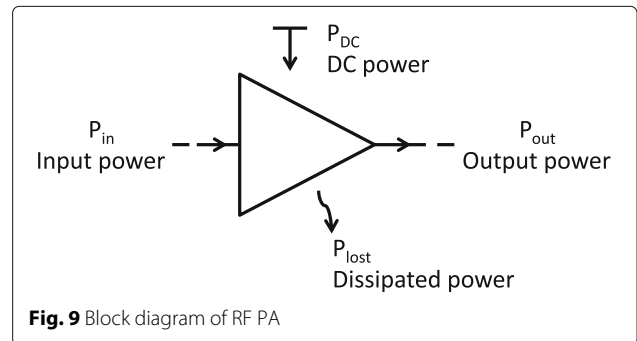
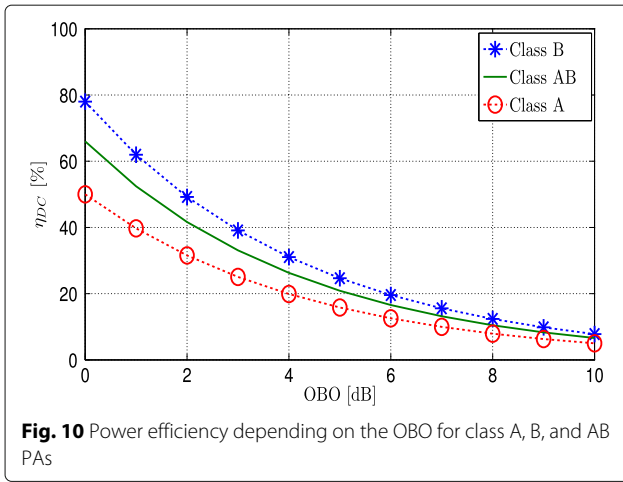


**Fig. 9** Block diagram of RF PA



is improved. Therefore, a trade-off between the PA efficiency and linearity must be considered. This aspect will be discussed in the next subsection.

## 5.2 Trade-off between PA linearity-efficiency and predistortion complexity considering clipping and predistortion

Wireless communication standards impose significant constraints on the transmitter's linearity, and at the same time require high efficiency. The EVM is a common figure of merits used to evaluate the linearity of communication systems and has become a mandatory part of some communication standards, e.g., [23]. In the rest of this subsection, we seek to maximize the power efficiency of the PA while respecting an EVM limitation and considering a given predistortion complexity.

In the first part, we investigate the PA linearity-efficiency trade-off. For this reason, we propose to control the clipping technique and adapt the transmit power in order to maximize the PA efficiency with respect to an EVM constraint. Therefore, we provide an analytical expression which gives the optimal input power back-off (IBO) and clipping threshold which must be taken to maximize the PA efficiency for any EVM constraint. In the next part, we investigate the complexity of the predistortion technique given that the complexity of the clipping technique is negligible compared to the complexity of the predistortion. So we propose to control the clipping and predistortion techniques in order to find the optimal configuration which maximizes the PA efficiency taking into account the predistortion complexity and satisfying the EVM constraint.

### 5.2.1 Control the clipping technique

From Eq. (30), we state that maximizing the efficiency is equivalent to minimizing the IBO. Consequently, we seek the minimum IBO and the corresponding clipping

threshold with respect to a specific EVM constraint. For this reason, we plot the EVM as a function of the IBO for different clipping thresholds using a DVB-T PA [33].

From Fig. 11, we remark that the EVM of the signal is constant if the  $IBO \geq PAPR_{[x_2]}$ ; however, it rapidly increases when the  $IBO < PAPR_{[x_2]}$ . According to the results of Theorem 4 represented in Fig. 11 and in agreement with [26], we can propose the following corollary of Theorem 4.

**Corollary 1** *The input power back-off (IBO) of the PA must be set identical to the PAPR of the signal after PAPR reduction in order to keep the maximum power efficiency gained by the PAPR reduction. Therefore, the analytical expression which gives the optimal IBO to maximize the PA efficiency with respect to an EVM constraint is given by*

$$\begin{aligned}
 EVM = & \left[ -2 \sum_{l=0}^{L_p-1} b_{2l+1} \sum_{q_1+\dots+q_{2K_p-1}=2l+1} \binom{2l+1}{q_1, \dots, q_{2K_p-1}} P_{x_1}^{\frac{s}{2}-1} \gamma \left( \frac{s+3}{2}, \lambda IBO \right) \right. \\
 & \times \prod_{k=0}^{K_p-1} (a_{2k+1})^{q_{2k+1}} - \frac{2H_{EQ}(A_{\max})}{\sqrt{P_{x_1}}} \left( \gamma \left( \frac{3}{2}, PAPR_{[x_1]} \right) - \gamma \left( \frac{3}{2}, \lambda IBO \right) \right) \\
 & + \sum_{p_1+\dots+p_{2L_p-1}=2} \binom{2}{p_1, \dots, p_{2L_p-1}} \prod_{l=0}^{L_p-1} (b_{2l+1})^{p_{2l+1}} \sum_{q_1+\dots+q_{2K_p-1}=m} \\
 & \times \binom{m}{q_1, \dots, q_{2K_p-1}} \times \gamma \left( \frac{s}{2} + 1, \lambda IBO \right) P_{x_1}^{\frac{s}{2}-1} \prod_{k=0}^{K_p-1} (a_{2k+1})^{q_{2k+1}} \\
 & - e^{-PAPR_{[x_1]}} \left( 1 + \frac{H_{EQ}(A_{\max})^2}{P_{x_1}} + PAPR_{[x_1]} \right) + 1 \\
 & + e^{-\lambda IBO} \left( \frac{H_{EQ}(A_{\max})^2}{P_{x_1}} \right) - 2 \sum_{l=0}^{L_p-1} b_{2l+1} \sum_{q_1+\dots+q_{2K_p-1}=2l+1} \\
 & \left. \times \binom{2l+1}{q_1, \dots, q_{2K_p-1}} P_{x_1}^{\frac{s}{2}-1} \gamma \left( \frac{s}{2} + 1, \lambda IBO \right) \prod_{k=0}^{K_p-1} (a_{2k+1})^{q_{2k+1}} \right]^{1/2}. \quad (31)
 \end{aligned}$$

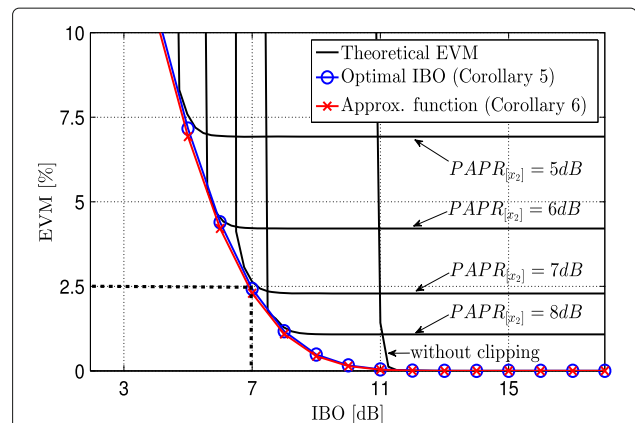


**Fig. 11** Theoretical EVM with predistortion as a function of the IBO using a DVB-T PA with  $L_p = 6$  and  $K_p = 5$  [33]. The analytical expression, which gives the optimal IBO for an EVM constraint given by Corollary 5, and the approximated one, given by Corollary 6, are also plotted

*Proof* According to the results of Theorem 4 represented in Fig. 11 and [26], we can state that the maximum possible power efficiency, avoiding PA saturation, is achieved when peak power of the amplified signal coincides with the saturation power. So by replacing the  $PAPR_{[x_2]}$  by the IBO in Eq. (25), we get Eq. (31).  $\square$

Equation 31 provides the optimal IBO which maximizes the PA efficiency with respect to an EVM constraint. As shown in Fig. 11, Eq. (31) provides an exact fitting to the optimal IBO. Thus, suppose now that one targets the maximum PA efficiency and wants to know which is the optimal IBO. However, there are two strategies to choose the optimal IBO. The first strategy aims at amplifying the transmit signal with no distortion which means that the EVM must be equal to zero. In this case, from the curve given by Fig. 11 according to Corollary 5, we remark that the optimal IBO which maximizes the PA efficiency and guaranties a null EVM is 11 dB. Thus, the clipping threshold should be also equal to 11 dB. On the other hand, the second strategy is to take advantage of the degree of freedom in the required EVM of the transmitted signal to boost the PA efficiency. Therefore, the key is to carefully manage the distortion, so we stay within the limits as specified in the communication standards [21–23]. For example, if the EVM constraint of the communication system is equal to 2.5%, from the curve given by Fig. 11 according to Corollary 5, we remark that the optimal IBO is 7 dB. Thus, the clipping threshold should be also equal to 7 dB. Referring to the characteristics of the used DVB-T PA in Fig. 12, we can state that the efficiency increases from 19.5 to 31% [33] by using the second strategy instead of the first one. So the efficiency gain is equal to 11.5% which is quite significant.

A simplification of Eq. (31) is given by the following corollary.

**Corollary 2** *The approximated analytical expression of (31), provided that the linearization process is sufficiently accurate, is given by*

$$EVM \approx \left[ -2\sqrt{\lambda IBO} \left( \gamma \left( \frac{3}{2}, PAPR_{[x_1]} \right) - \gamma \left( \frac{3}{2}, \lambda IBO \right) \right) e^{-\lambda IBO} (2\lambda IBO + 1) - e^{-PAPR_{[x_1]}} (PAPR_{[x_1]} + \lambda IBO + 1) \right]^{1/2} \tag{32}$$

*Proof* If the linearization technique is sufficiently accurate, the distortion of the PA could be negligible compared to the clipping distortion. Therefore, the expression of the EVM can be approximated by neglecting the integral  $I_9$  in Eq. (58) and assuming that  $\frac{H_{EQ}(A_{max})^2}{P_{x1}} = \lambda PAPR_{[x_2]}$ . Moreover, according to Corollary 1,  $PAPR_{[x_2]} = IBO$ , so after doing some maths we obtain Eq. (32).  $\square$

From Fig. 11, we show that Corollary 2 provides a perfect approximation of Corollary 1. We remark that the approximated EVM given by Eq. (32) is slightly less than the exact one given by Eq. (31). This is explained by the considered simplification of the PA distortion. Indeed, the importance of Corollary 2 is that it does not depend on the linearization technique. So, for any linearization technique, using the clipping as a PAPR reduction, Corollary 2 is valid. However, the less accurate the used linearization technique is, the less correct the approximation is.

**5.2.2 Control the clipping and predistortion techniques**

In this part, we aim at jointly controlling the clipping and predistortion techniques in order to perform an optimal

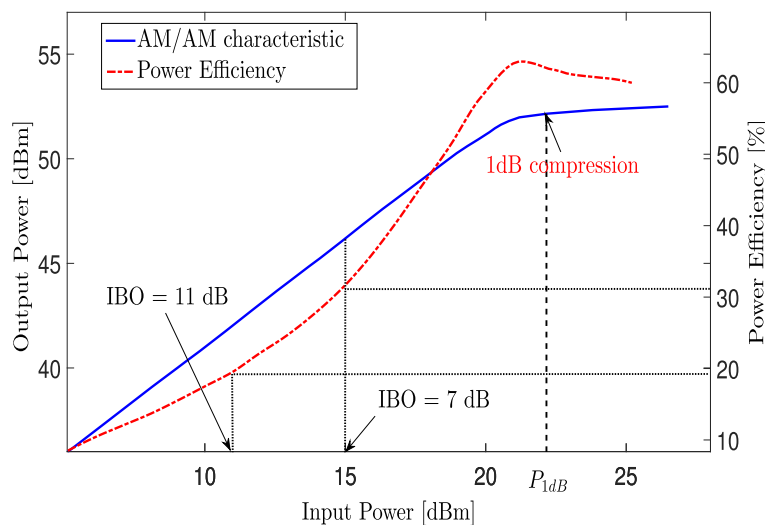


**Fig. 12** The output power and power efficiency of the DVB-T PA versus the input power [33]

configuration which maximizes the PA efficiency taking into account the predistortion complexity and satisfying the EVM constraint. For this reason, we investigate the complexity of the predistortion and seek a compromise between the complexity and linearity. Referring to Eq. (11), it can be rewritten in a matrix format as

$$\mathbf{X}_{N \times 1} = \mathbf{R}_{N \times K_p} \mathbf{A}_{K_p \times 1}, \tag{33}$$

where  $\mathbf{X}_{N \times 1}$  represents the predistortion output vector and  $\mathbf{R}_{N \times K_p}$  is the matrix which contains all the linear and product terms of the amplitude signal  $r, r^3, \dots, r^{2k+1}$  for all the input data samples. Note that  $N$  represents the number of used input/output data samples and  $K_p$  is the number of involved predistortion coefficients.  $\mathbf{A}_{K_p \times 1}$  represents the unknown coefficients vector.

To extract the coefficients, the indirect learning [34] is used, where the predistorted output signal,  $x_3(n)$ , is used as the expected output, while the output of the PA,  $z(n)$ , is used as the input of the model. Using the least square algorithm, the coefficients vector can be estimated from

$$\hat{\mathbf{A}}_{K_p \times 1} = \left[ (\mathbf{Z}_{N \times K_p})^H \mathbf{Z}_{K_p \times N} \right]^{-1} (\mathbf{Z}_{N \times K_p})^H \mathbf{X}_{N \times 1}, \tag{34}$$

where  $\mathbf{Z}$  is the PA output matrix in a similar form to the matrix  $\mathbf{R}$ , and  $(\cdot)^H$  represents the Hermitian transpose. Now, we have to compute the computational complexity of the matrix operations in Eq. (34). Indeed, there are one matrix inversion and three matrix-matrix multiplications. In fact, the inversion of a  $K_p \times K_p$  matrix is approximately equivalent to  $K_p^3$  number of multiplication operations. However, multiplying a  $K_p \times N$  matrix by a  $N \times K_p$  matrix requires  $(N - 1) \times K_p \times K_p$  additions and  $K_p \times N \times K_p$  multiplications.

Therefore, the total number of multiplication operations and addition operations to be conducted in Eq. (34) are given respectively by

$$O_{N, K_p}^{\otimes} = N \times K_p^2 \times 2 + N \times K_p + K_p^3, \tag{35}$$

$$O_{N, K_p}^{\oplus} = (N - 1) \times K_p^2 + N \times (K_p - 1) \times K_p + (N - 1) \times K_p. \tag{36}$$

This leads to the conclusion that the computational complexity of model extraction actually depends on the nonlinear model order of the predistortion  $K_p$  and the number of the training samples  $N$ . Thereby, the more we decrease the number of predistortion coefficients and the training samples, the more we decrease the computational complexity. Consequently, thanks to our EVM expressions we can minimize the computational complexity of the predistortion technique by controlling  $K_p$ . Thus, we have to choose the minimum number of coefficients with respect to our EVM constraint.

To discuss this issue, we plot Eq. (31) to find the optimal IBO for different predistortion orders. Note again that Eq. (31) gives the optimal IBO and clipping threshold which must be taken to maximize the PA efficiency for any EVM constraint. Based on the foregoing, the more we decrease the clipping threshold and the IBO, the more the PA efficiency increases. Furthermore, the more we decrease the predistortion order, the more the computational complexity decreases. On the other hand, we remark from Fig. 13 that the more we decrease the predistortion order, the more the EVM increases. Consequently, assuming for example that the EVM should be less than 2.5%, we notice from Fig. 13 that different solutions can be adopted according to the transmission constraints and

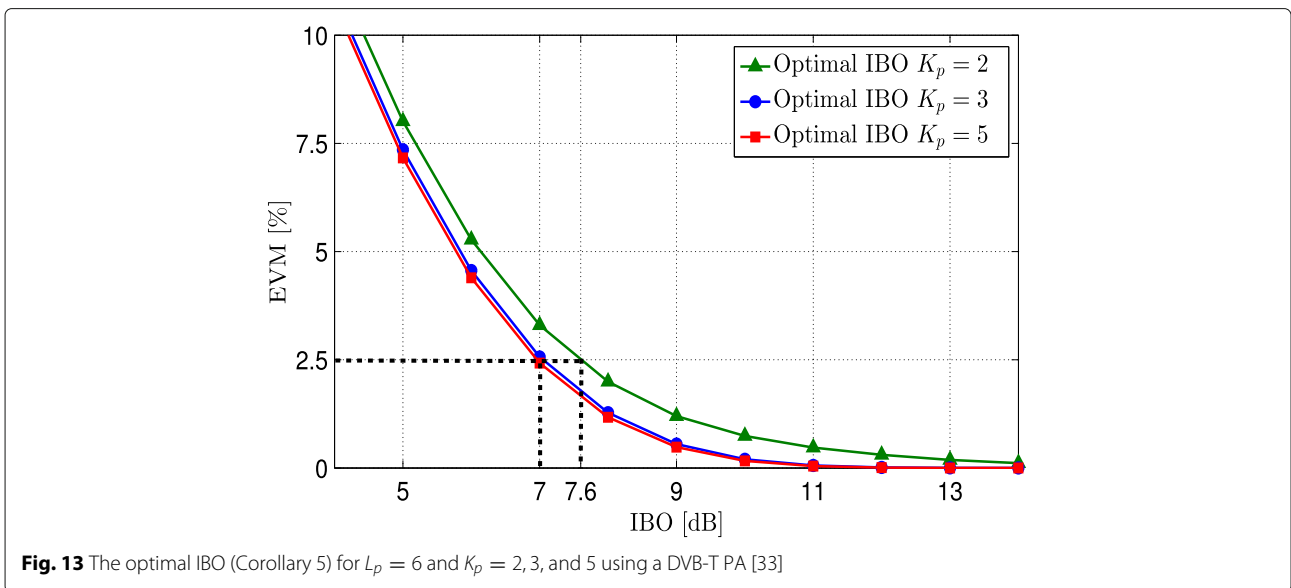


Fig. 13 The optimal IBO (Corollary 5) for  $L_p = 6$  and  $K_p = 2, 3,$  and  $5$  using a DVB-T PA [33]

limits. So, in terms of PA efficiency and without taking into account the predistortion complexity, the optimal IBO, with respect to the EVM constraint, is 7 dB which implies a  $\text{PAPR}_{[x_2]} = 7$  dB. However, if we do not have sufficient computational capacity for the predistortion technique, we can decrease the predistortion order and choose for example  $K_p = 2$  instead of choosing  $K_p = 5$ . In this case, the optimal IBO, that satisfies the computational complexity and respects the EVM constraint, becomes 7.6 dB. Although the PA efficiency decreases from 32 to 30%, we significantly mitigate the predistortion complexity. Therefore, the number of multiplication operations decreases from  $55N + 125$  to  $10N + 8$  and the number of addition operations decreases from  $50N - 30$  to  $8N - 6$ . So thanks to our proposed theorems, we can decrease, in this scenario, the number of multiplication operations five times and the number of addition operations six times.

### 6 Conclusions

In this paper, the EVM expression of a multicarrier signal distorted by a polynomial PA model is derived with or without the use of a clipping technique. Then, the impact of a polynomial predistortion on the EVM expressions is investigated. The provided analytical expressions of the EVM are based on series expansions, and depend on the PA characteristics and the predistortion characteristics, as well as the PAPR and the average power of both input and clipped signals. Simulation results compared to our proposed model confirm the accuracy of our derived analytical expressions. Therefore, it is no more necessary to realize a PA prototype to know if it respects the EVM standard. This analytical expression could be favorably integrated in simulation models to validate the PAs behavior. Moreover, the trade-off between the PA linearity and efficiency is discussed. We showed that our theoretical EVM expressions are very useful for optimizing transmitter efficiency and linearity. Indeed, an analytical expression which gives the optimal IBO maximizing the PA efficiency with respect to any EVM constraint is provided. Then, the complexity of the predistortion technique is investigated aiming at reducing it.

It is worthwhile to note that our proposed theoretical analyses could be very useful for optimizing future transmitter efficiency and linearity and the computational complexity of the predistortion technique. These analytical results are very interesting and could be applied in the field of broadcasting for the deployment of DVB-T2 transmitters as well as in LTE cellular networks. Future works should investigate out-of-band distortions, e.g., adjacent channel power ratio (ACPR), and take into account the memory effects of the PA.

### Endnote

<sup>1</sup>Note that the odd order comes from the bandpass assumption as explained in [32] p. 161.

### Appendix 1: Proof of the EVM derivation when clipping and predistortion are deactivated

In this case, using Eqs. (3), (10), and (13), the second order moment of the magnitude error, denoted by  $m_2$ , can be expressed as follows

$$m_2 = \int_0^{R_{\max}} |H_{PA}(r) - r|^2 f_{x_1}(r) dr$$

$$= \int_0^{R_{\max}} \left| \sum_{l=0}^{L_p-1} C_{2l+1} r^{2l+1} \right|^2 \frac{2r}{P_{x_1}} e^{-\frac{r^2}{P_{x_1}}} dr, \quad (37)$$

where

$$C_{2l+1} = \begin{cases} b_1 - 1 & \text{if } l = 0 \\ b_{2l+1} & \text{if } l \neq 0. \end{cases} \quad (38)$$

According to the multinomial theorem, it is possible to expand the squared term in Eq. (37) in the form of products of powers. In fact, for any positive integer  $m$  and any nonnegative integer  $n$ , the multinomial formula is given by

$$(x_1 + x_2 + \dots + x_m)^n = \sum_{p_1 + \dots + p_m = n} \binom{n}{p_1, p_2, \dots, p_m} \prod_{i=1}^m x_i^{p_i}, \quad (39)$$

where

$$\binom{n}{p_1, p_2, \dots, p_m} = \frac{n!}{p_1! p_2! \dots p_m!} \quad (40)$$

is a multinomial coefficient. The sum in Eq. (39) is taken over all combinations of nonnegative integer exponents  $p_1$  through  $p_m$  such that the sum of all  $p_i$  is  $n$ . That is, for each term in the expansion, the exponents of the  $x_i$  must add up to  $n$ . Hence, we can obtain an expansion of  $m_2$  as

$$m_2 = \sum_{p_1 + \dots + p_{L_p-1} = 2} \binom{2}{p_1, \dots, p_{L_p-1}}$$

$$\times \prod_{l=0}^{L_p-1} (C_{2l+1})^{p_{2l+1}} \int_0^{R_{\max}} \frac{2r^s}{P_{x_1}} e^{-\frac{r^2}{P_{x_1}}} dr \quad (41)$$

with

$$s = \sum_{l=0}^{L_p-1} (2l + 1) p_{2l+1} + 1. \quad (42)$$

Noting that the integral in Eq. (41) is of the form of the incomplete gamma function which is defined as

$$\gamma(\alpha, u) = \int_0^u x^{\alpha-1} e^{-x} dx. \quad (43)$$

Then, using Eq. (12), the EVM expression can be written as Eq. (14).

**Appendix 2: Proof of the EVM derivation when clipping is activated**

Using Lemma 1 and Eq. (13), the second order moment of the magnitude error is given by

$$m_2 = \underbrace{\int_0^{A_{\max}} |r - H_{PA}(r)|^2 f_{x_1} dr}_{I_1} + \underbrace{\int_{A_{\max}}^{R_{\max}} |r - H_{PA}(A_{\max})|^2 f_{x_1} dr}_{I_2}. \quad (44)$$

At first, the derivation of  $I_1$  is similar to derivation of  $m_2$  in the case without clipping which is previously presented. Thus, using Lemma 2,  $I_1$  can be computed as

$$I_1 = P_{x_1} \frac{s-1}{2} \sum_{p_1+\dots+p_{2L_p-1}=2} \binom{2}{p_1, \dots, p_{2L_p-1}} \times \prod_{l=0}^{L_p-1} (C_{2l+1})^{p_{2l+1}} \times \gamma\left(\frac{s+1}{2}, \lambda \text{PAPR}_{[x_2]}\right). \quad (45)$$

However,  $I_2$  is an integral to be calculated. After expanding the squared term in  $I_2$  and letting  $u = \frac{r^2}{P_{x_1}}$  we get

$$I_2 = P_{x_1} \underbrace{\int_{\lambda \text{PAPR}_{[x_2]}}^{\text{PAPR}_{[x_1]}} u e^{-u} du}_{I_3} - 2H_{PA}(A_{\max}) \sqrt{P_{x_1}} \underbrace{\int_{\lambda \text{PAPR}_{[x_2]}}^{\text{PAPR}_{[x_1]}} \sqrt{u} e^{-u} du}_{I_4} + H_{PA}(A_{\max})^2 \underbrace{\int_{\lambda \text{PAPR}_{[x_2]}}^{\text{PAPR}_{[x_1]}} e^{-u} du}_{I_5}. \quad (46)$$

By applying integration by parts and using Lemma 2,  $I_3$  and  $I_5$  can be written as

$$I_3 = P_{x_1} e^{-\lambda \text{PAPR}_{[x_2]}} (\lambda \text{PAPR}_{[x_2]} + 1) - P_{x_1} e^{-\text{PAPR}_{[x_1]}} (\text{PAPR}_{[x_1]} + 1), \quad (47)$$

$$I_5 = H_{PA}(A_{\max})^2 (e^{-\lambda \text{PAPR}_{[x_2]}} - e^{-\text{PAPR}_{[x_1]}}). \quad (48)$$

Then, using the integral identity in Eq. (43),  $I_4$  can be calculated as

$$I_4 = -2\sqrt{P_{x_1}} H_{PA}(A_{\max}) \left( \gamma\left(\frac{3}{2}, \text{PAPR}_{[x_1]}\right) - \gamma\left(\frac{3}{2}, \lambda \text{PAPR}_{[x_2]}\right) \right). \quad (49)$$

Finally, compiling  $I_1$  and  $I_2$ , the EVM expression can be written as Eq. (18).

**Appendix 3: Proof of the EVM derivation when predistortion is activated**

In this case, using Eqs. (13) and (20), the second-order moment of the magnitude error can be calculated as follows

$$m_2 = \int_0^{R_{\max}} |H_{EQ}(r) - r|^2 f_{x_1}(r) dr = \int_0^{R_{\max}} \left| \sum_{l=0}^{L_p-1} b_{2l+1} \left[ \sum_{k=0}^{K_p-1} a_{2k+1} r^{2k+1} \right]^{2l+1} - r \right|^2 f_{x_1}(r) dr. \quad (50)$$

After expanding the squared term in Eq. (50), we get

$$m_2 = \underbrace{\int_0^{R_{\max}} r^2 \frac{2r}{P_{x_1}} e^{-\frac{r^2}{P_{x_1}}} dr}_{I_6} - 2 \underbrace{\int_0^{R_{\max}} r \sum_{l=0}^{L_p-1} b_{2l+1} \left[ \sum_{k=0}^{K_p-1} a_{2k+1} r^{2k+1} \right]^{2l+1} \frac{2r}{P_{x_1}} e^{-\frac{r^2}{P_{x_1}}} dr}_{I_7} + \underbrace{\int_0^{R_{\max}} \left( \sum_{l=0}^{L_p-1} b_{2l+1} \left[ \sum_{k=0}^{K_p-1} a_{2k+1} r^{2k+1} \right]^{2l+1} \right)^2 \frac{2r}{P_{x_1}} e^{-\frac{r^2}{P_{x_1}}} dr}_{I_8}. \quad (51)$$

In fact, the computation of  $I_6$  is easily obtained by applying integration by parts

$$I_6 = -P_{x_1} (e^{-\text{PAPR}_{[x_1]}} (\text{PAPR}_{[x_1]} + 1) - 1). \quad (52)$$

Then, using the multinomial theorem, we can expand the power term in  $I_7$ , and after integration we have

$$I_7 = -2 \sum_{l=0}^{L_p-1} b_{2l+1} \sum_{q_1+q_3+\dots+q_{2K_p-1}=2l+1} \binom{2l+1}{q_1, q_3, \dots, q_{2K_p-1}} \times P_{x_1}^{\frac{s}{2}} \gamma\left(\frac{s}{2} + 1, \text{PAPR}_{[x_1]}\right) \prod_{k=0}^{K_p-1} (a_{2k+1})^{q_{2k+1}}, \quad (53)$$

with

$$s = \sum_{k=0}^{K_p-1} (2k+1) q_{2k+1} + 1. \quad (54)$$



Likewise, we apply the multinomial theorem twice to the squared term in  $I_8$ , and after integration we get

$$\begin{aligned}
 I_8 = & \sum_{p_1+p_3+\dots+p_{2L_p-1}=2} \binom{2}{p_1, p_3, \dots, p_{2L_p-1}} \prod_{l=0}^{L_p-1} (b_{2l+1})^{p_{2l+1}} \\
 & \times \sum_{q_1+q_3+\dots+q_{2K_p-1}=m} \binom{m}{q_1, q_3, \dots, q_{2K_p-1}} \prod_{k=0}^{K_p-1} (a_{2k+1})^{q_{2k+1}} \\
 & \times P_{x_1}^{\frac{n}{2}} \gamma \left( \frac{n}{2} + 1, \text{PAPR}_{[x_1]} \right), \tag{55}
 \end{aligned}$$

where

$$m = \sum_{l=0}^{L_p-1} p_{2l+1} (2l + 1), \tag{56}$$

$$n = \sum_{k=0}^{K_p-1} (2k + 1) q_{2k+1}. \tag{57}$$

Finally, after compiling these integrals, the EVM expression can be expressed as Eq. (21).

#### Appendix 4: Proof of the EVM derivation when clipping and predistortion are activated

Using Lemma 1, Eq. (13), and Eq. (20), the second-order moment of the magnitude error can be written as

$$\begin{aligned}
 m_2 = & \underbrace{\int_0^{A_{\max}} |H_{EQ}(r) - r|^2 f_{x_1} dr}_{I_9} \\
 & + \underbrace{\int_{A_{\max}}^{R_{\max}} |H_{EQ}(A_{\max}) - r|^2 f_{x_1} dr}_{I_{10}}. \tag{58}
 \end{aligned}$$

However, the derivation of  $I_9$  is similar to the derivation of Eq. (50). Moreover, the derivation of  $I_{10}$  is previously presented, which is exactly the same calculation of  $I_2$ . Hence, the EVM expression can be expressed as Eq. (25).

#### Author details

<sup>1</sup>IETR/INSA de Rennes, 20 Ave. des Buttes de Coësmes, Rennes, France. <sup>2</sup>IETR/CentraleSupélec, Campus de Rennes, Cesson-Sévigne, France.

Received: 5 May 2016 Accepted: 10 November 2016

Published online: 07 December 2016

#### References

1. R Yoshizawa, H Ochiai, in *IEEE 82nd Vehicular Technology Conference (VTC Fall), Boston, USA*. Effect of clipping and filtering with distortionless PAPR reduction for OFDM systems, (2015), pp. 1–5. doi:10.1109/VTCFall.2015.7390907
2. KG Paterson, in *Personal, Indoor and Mobile Radio Communications, 1998. The Ninth IEEE International Symposium on*. Coding techniques for power controlled OFDM, vol. 2 (1998), pp. 801–805. doi:10.1109/PIMRC.1998.734673
3. RW Bauml, RFH Fischer, JB Huber, Reducing the peak-to-average power ratio of multicarrier modulation by selected mapping. *Electronics Letters*. **32**(22), 2056–2057 (1996). doi:10.1049/el:19961384
4. Tellado-Mourelo, *Peak to Average Power Reduction for Multicarrier Modulation*. (Ph.D. Thesis, Stanford University. Dept. of Electrical Engineering, 2000)
5. BS Krongold, DL Jones, PAR reduction in OFDM via active constellation extension. *Broadcasting, IEEE Transactions on*. **49**(3), 258–268 (2003). doi:10.1109/TBC.2003.817088
6. A Bo, Y Zhi-Xing, P Chang-Yong, Z Tao-Tao, W Yong, G Jian-Hua, Improved LUT Technique for HPA Nonlinear Pre-Distortion in OFDM Systems. *Wireless Personal Communications*. **38**(4), 495–507 (2006). doi:10.1007/s11277-006-9062-5
7. DC Cox, Linear Amplification with Nonlinear Components. *Communications, IEEE Transactions on*. **22**(12), 1942–1945 (1974). doi:10.1109/TCOM.1974.1092141
8. PB Kenington, *High Linearity RF Amplifier Design*, 1st edn. (Artech House, Inc., Norwood, MA, 2000)
9. R Sperlrich, Y Park, G Copeland, JS Kenney, in *Microwave Symposium Digest, 2004 IEEE MTT-S International*. Power amplifier linearization with digital pre-distortion and crest factor reduction, vol. 2 (2004), pp. 669–672. doi:10.1109/MWSYM.2004.1336077
10. JS Kenney, JH Chen, in *2006 IEEE International Conference on Microwaves, Radar Wireless Communications*. Power amplifier linearization and efficiency improvement techniques for commercial and military applications, (2006), pp. 3–8. doi:10.1109/MIKON.2006.4345092
11. H-G Ryu, Y-H Lee, A new combined method of the block coding and predistortion for the nonlinear distortion compensation. *Consumer Electronics, IEEE Transactions on*. **49**(1), 27–31 (2003). doi:10.1109/TCE.2003.1205452
12. H-G Ryu, TP Hoa, KM Lee, S-W Kim, J-S Park, Improvement of power efficiency of HPA by the PAPR reduction and predistortion. *Consumer Electronics, IEEE Transactions on*. **50**(1), 119–124 (2004). doi:10.1109/TCE.2004.1277850
13. M Brandon, M Ariaudo, S Traverso, J Bouvier, I Fijalkow, JL Gautier, in *IEEE 9th International New Circuits and Systems Conference (NEWCAS), Bordeaux, France*. Linearity improvement thanks to the association of Active Constellation Extension and digital predistortion for OFDM, (2011), pp. 293–296. doi:10.1109/NEWCAS.2011.5981313
14. BS Krongold, DL Jones, PAR reduction in OFDM via active constellation extension. *Broadcasting, IEEE Transactions on*. **49**(3), 258–268 (2003). doi:10.1109/TBC.2003.817088
15. T Miracco, in *Solid-State and Integrated-Circuit Technology, ICSICT 2008, Beijing, China. 9th International Conference on*. Crest factor reduction and digital pre-distortion for wireless RF power amplifier optimization, (2008), pp. 1357–1360. doi:10.1109/ICSICT.2008.4734813
16. L-C Chang, C-H Yang, in *7th International Conference on Information, Communications and Signal Processing, ICICIS, Taiwan*. A combined approach of MBAP/PR PAPR reduction and polynomial predistortion for performance enhancement, (2009), pp. 1–5. doi:10.1109/ICICIS.2009.5397641
17. S Hu, G Wu, Q Wen, Y Xiao, S Li, Nonlinearity Reduction by Tone Reservation with Null Subcarriers for WiMAX System. *Wireless Personal Communications*. **54**(2), 289–305 (2010). doi:10.1007/s11277-009-9726-z
18. RN Braithwaite, in *Integrated Nonlinear Microwave and Millimetre-Wave Circuits (INMMIC), Ireland. Workshop On*. Implementing crest factor reduction (CFR) by offsetting digital predistortion (DPD) coefficients, (2012), pp. 1–3. doi:10.1109/INMMIC.2012.6331928
19. S Hu, G Wu, J-J Ping, S-Q Li, in *Circuits and Systems for Communications, ICCSC, Shanghai, China. 4th IEEE International Conference on*. HPA Nonlinearity Reduction by Joint Predistorter and Tone-Reservation with Null Subcarriers in WiMAX Systems, (2008), pp. 187–190. doi:10.1109/ICCSC.2008.46
20. S Ragusa, J Palicot, Y Louët, C Lereau, in *International Conference on Telecommunications (ICT) 2006*. Invertible Clipping for Increasing the Power Efficiency of OFDM Amplification, (Funchal, Portugal, 2006), pp. 1–6. https://hal.archives-ouvertes.fr/hal-00083987
21. IEEE-SA Standards Board, IEEE Standard for Telecommunications and Information Exchange Between Systems - LAN/MAN Specific Requirements. IEEE 802.11a (2012) (1999)

22. IEEE-SA Standards Board, IEEE Standard for Local and Metropolitan Area Networks, Part 16, Amendment 2. IEEE 802.16e (2009) (2005)
23. European Telecommunications Standards Institute, LTE; Evolved Universal Terrestrial Radio Access (E-UTRA); Base Station (BS) Radio Transmission and Reception. 3GPP TS 36.104 version 11.2.0 Release 11 (2012)
24. A Cheaito, M Crussiere, Y Louet, J-F Helard, in *Vehicular Technology Conference (VTC Spring), Glasgow, Scotland, 2015 IEEE 81st*. EVM Derivation for Multicarrier Signals: Joint Impact of Non-Linear Amplification and Predistortion, (2015), pp. 1–6. doi:10.1109/VTCSpring.2015.7145831
25. A Cheaito, J-F Helard, M Crussiere, Y Louet, Impact of Clipping on EVM of the Predistorted Non-Linear Amplified Multicarrier Signals. The Twelfth International Symposium on Wireless Communication Systems, Brussels, Belgium, 1–5 (2015)
26. OA Gouba, Y Louet, in *European Wireless, Poznan, Poland. 18th European Wireless Conference*. Theoretical analysis of the trade-off between efficiency and linearity of the high power amplifier in OFDM context, (2012), pp. 1–7
27. OA Gouba, Y Louet, in *Wireless Communications and Networking Conference (WCNC) Paris, France, 2012 IEEE*. Predistortion performance considering peak to average power ratio reduction in OFDM context, (2012), pp. 204–208. doi:10.1109/WCNC.2012.6214128
28. I Kotzer, S Har-Nevo, S Sodin, S Litsyn, An Analytical Approach to the Calculation of EVM in Clipped Multi-Carrier Signals. *Communications, IEEE Transactions on*. **60**(5), 1371–1380 (2012). doi:10.1109/TCOMM.2012.12.100447
29. RJ Baxley, C Zhao, GT Zhou, Constrained clipping for crest factor reduction in OFDM. *IEEE Transactions on Broadcasting*. **52**(4), 570–575 (2006). doi:10.1109/TBC.2006.883301
30. I Kotzer, S Har-Nevo, S Sodin, S Litsyn, in *Electrical and Electronics Engineers in Israel (IEEEI), 2010 IEEE 26th Convention of*. An analytical approach to the calculation of evm in clipped OFDM signals, (2010), pp. 000193–000197. doi:10.1109/IEEEI.2010.5661957
31. P Banelli, G Leus, GB Giannakis, in *Signal Processing Conference, 2002 11th European, Toulouse, France*. Bayesian estimation of clipped Gaussian processes with application to OFDM, (2002), pp. 1–4
32. MC Jeruchim, P Balaban, KS Shanmugan (eds.), *Simulation of Communication Systems: Modeling, Methodology and Techniques*, 2nd edn. (Kluwer Academic Publishers, Norwell, MA, 2000)
33. NXP Semiconductors, AN10945 174 MHz to 230 MHz DVB-T power amplifier with the BLF881. Technical report (2010). [www.ampleon.com/documents/application-note/AN10945.pdf](http://www.ampleon.com/documents/application-note/AN10945.pdf)
34. L Ding, R Raich, GT Zhou, in *2002 IEEE International Conference on Acoustics, Speech, and Signal Processing (ICASSP), Orlando, Florida, USA*. A hammerstein predistortion linearization design based on the indirect learning architecture, vol. 3 (2002), pp. 2689–2692. doi:10.1109/ICASSP.2002.5745202
35. MA Imran, P Partners, *Energy efficiency analysis of the reference systems, areas of improvements and target breakdown. Technical report*. (EARTH Project Report, Deliverable D2.3, 2012)
36. MK Kazimierzczuk, *RF Power Amplifiers*. (Wright State University, Dayton, Ohio, USA, A John Wiley and Sons, Ltd., Publication, 2008)

Submit your manuscript to a SpringerOpen<sup>®</sup> journal and benefit from:

- Convenient online submission
- Rigorous peer review
- Immediate publication on acceptance
- Open access: articles freely available online
- High visibility within the field
- Retaining the copyright to your article

---

Submit your next manuscript at ► [springeropen.com](http://springeropen.com)

---